Radiation Physics and Chemistry xxx (xxxx) xxx–xxx

Contents lists available at ScienceDirect

Radiation Physics and Chemistry

journal homepage: www.elsevier.com/locate/radphyschem

Formation and growth of Pd nanoparticles in UiO-67 MOF by in situ EXAFS

E.G. Kamyshova[a], A.A. Skorynina[a], A.L. Bugaev[a,*], C. Lamberti[a,b], A.V. Soldatov[a]

[a] The Smart Materials Research Institute, Southern Federal University, Rostov-on-Don, Russia
[b] Department of Physics, University of Turin, Turin, Italy

ARTICLE INFO

Keywords:
Metal-organic frameworks
UiO-67
Pd nanoparticles
EXAFS

ABSTRACT

We present a detailed extended X-ray absorption fine structure (EXAFS) characterization of the formation process of palladium nanoparticles (NPs) inside UiO-67 metal-organic framework (MOF). Starting from the initial UiO-67 structure with 10% of $PdCl_2$bpydc moieties with grafted Pd ions replacing standard 4,4′-biphenyldicarboxylate linkers, we followed *in situ* H_2-temperature programmed reduction (TPR) of the material. The cleavage of Pd–N and Pd–Cl bonds and simultaneous growth of the Pd–Pd contribution of metal NPs start at 200 °C. Below 300 °C metal NPs are small and are constrained inside the cavities of UiO-67, while at higher temperatures, the Pd–Pd coordination number (CN) increases to its bulk values, implying the aggregation of NPs into big palladium particles with probable destruction of MOF crystal structure. The formation of bigger particles is also confirmed by non-linear dependence of Debye-Waller parameter (DW) for Pd–Pd contribution upon temperature.

1. Introduction

Synthesis of new metal-organic frameworks (MOFs) and studies of their structure and properties have been intensively performed during last two decades. MOFs are constructed from inorganic cornerstones connected by organic linkers (Butova et al., 2016). These structures demonstrate exceptional porosity with high specific surface area and pore volume. MOFs find versatile applications as drug-delivery agents and sensors, in gas storage and separation systems, and in catalysis. However, catalytic activity of MOFs is limited by the fact that metal atoms inside inorganic cornerstones usually do not have coordination vacancies. Additional useful properties can be obtained by the functionalization of MOFs by metals (Wang and Cohen, 2009), which allows combining unique porosity of MOFs with high catalytic activity of metals. Functionalization of linkers by metal ions have been successfully adopted for UiO-67 MOF, a structure with high chemical, thermal and mechanical stabilities that encourage its applications in catalysis (Cavka et al., 2008; Chavan et al., 2012). Although MOFs are crystalline materials extensively studied by X-ray diffraction techniques, X-ray absorption spectroscopies (XAS) play a primary role in determining the local structure around active metal sites in such structures (Bordiga et al., 2010; Soldatov et al., 2018). In particular, in our previous studies (Borfecchia et al., 2017; Braglia et al., 2017a, 2017b, 2017c; Øien et al., 2015), Pt and Cu-functionalized UiO-67 MOFs have been characterized by *in situ* XAS to show their local coordination, geometry, redox properties and structure-reactivity relationships.

In this work, we focus on the detailed characterization of the evolution of local structure around Pd-atoms in Pd-functionalized UiO-67 MOF by *in situ* Pd *K*-edge extended X-ray absorption fine structure (EXAFS) spectroscopy. Simultaneous analysis of the whole temperature evolution of EXAFS spectra and application of constrains to the temperature-dependence of structural parameters allowed us to track the transition of Pd ions from the linkers into small Pd nanoparticles (NPs) stabilized inside the cavities of UiO-67 and their further agglomeration to bigger Pd particles with possible destruction of MOF crystal structure during H_2 temperature programmed reduction (H_2-TPR). The obtained coordination numbers (CNs), Debye-Waller factors (DW) and interatomic distances for Pd–N, Pd–Cl, and Pd–Pd contributions during H_2-TPR are reported.

2. Experimental and methods

UiO-67 MOFs were functionalized by palladium via pre-made linker synthesis (PMLS) approach as described elsewhere (Bugaev et al., 2018). The samples were pressed into a pellet to optimize the absorption step at Pd *K*-edge. *In situ* EXAFS measurements in transmission mode during H_2-TPR were performed at BM23 beamline of ESRF. The spectra were collected till $k = 14$ Å^{-1}. The pellet was loaded inside the microtomo cell (Bellet et al., 2003) allowing us to control the sample temperature and atmosphere. The sample was heated in a flow of 5% H_2 in helium from room temperature (RT) to 450 °C by 3 °C/min. In total

* Corresponding author.
E-mail address: abugaev@sfedu.ru (A.L. Bugaev).

https://doi.org/10.1016/j.radphyschem.2019.02.003
Received 29 September 2018; Received in revised form 7 November 2018; Accepted 1 February 2019
Available online 02 February 2019
0969-806X/

10 subsequent spectra were collected during the temperature ramp.

Demeter software package (Ravel and Newville, 2005) was used to process and analyze EXAFS spectra. Fourier analysis was performed simultaneously for the whole series of spectra. This allowed us to reduce the number of independent variables by using common variables and applying several constrains described in the Results and discussions section. The 3.0–13.0 $Å^{-1}$ Δk interval was used for all spectra. For ΔR, 1.0–2.4 Å interval was used for the spectra up to 200 °C, and 1.0–3.0 Å for higher temperatures. The S_0^2 value was fixed at 0.80 as determined for Pd foil.

3. Results and discussion

Fourier-transformants (FTs) of EXAFS spectra shown in Fig. 1a indicate the following main trends observed during H_2-TPR. The initial spectrum (black curve) is characterized by a double peak in the 1.2–2.3 Å interval (phase-uncorrected), originated from the square planar local coordination of Pd atoms with two neighboring nitrogen and two chlorine atoms. Above 200 °C (orange curve), the Pd—Cl and Pd—N contributions diminish, and a new feature appears around 2.6 Å (phase-uncorrected), assigned to Pd—Pd contribution from Pd NPs which are starting to be formed at this temperature. Finally, in the last spectrum (blue curve), only Pd–Pd peak is left.

The quantitative Fourier-analysis of the spectra presented in Fig. 1a requires a big number of parameters to be taken into consideration. In particular, CNs, σ^2 and interatomic distances for Pd–N, Pd–Cl, and Pd–Pd contributions already require 9 parameters with additional two different zero energy corrections (ΔE_0) for Pd^{2+} and Pd^0 states, and relative fraction of Pd in each of these states. This means that for the spectra where all three contributions coexist, simultaneous fitting of 12 parameters is needed, while the number of independent points (N_{idp}) for the used Δk and ΔR interval is below 9.

To reduce the number of independent fitting parameters the whole series of experimental data were analyzed simultaneously applying several constrains described in the following. For both Pd–N and Pd–Cl contributions, the ΔE_0 and interatomic distances were assumed to be the same in the whole temperature range. Although this may not be fullfilled if, for example, one Cl-atom is detached from Pd, the made assumption resulted in a good fitting quality. Correlated Debye model was used to consider the temperature dependence of the DW parameters for Pd–N and Pd–Cl. Finally, the temperature evolutions $N(T)$ of Pd–N and Pd–Cl CNs were assumed to have a sigmoid shape given by the Eq. (1):

$$N(T) = \frac{N_0}{1+e^{(T-T_0)/\tau}} \quad (1)$$

where N_0 is a starting value of CNs, T is the temperature of current spectrum, and the decrease of N is spanned over the interval proportional to τ, centered at T_0. Thus, only 10 parameters were used to describe the evolution of Pd–N and Pd–Cl in the whole series of spectra: ΔE_0, R_{Pd-N}, R_{Pd-Cl}, $DebyeT_N$, $DebyeT_{Cl}$, N_0, $T_{0,N}$, $T_{0,Cl}$, τ_N, and τ_{Cl}. N_0 was common for both Pd–N and Pd–Cl CNs and its refined value was $N_0 = 1.95 \pm 0.08$, which is close to the expected value of 2.

For Pd–Pd contributions, we were forced to use independent R_{Pd-Pd}, N_{Pd}, $\Delta E_{0,Pd}$, and σ^2_{Pd} for each temperature for the following reasons. First, the increase of Pd–Pd CNs did not follow a similar to Eq. (1) evolution due to the fact that the Pd particles had two stages of grows (vide infra). Then, the changes in the size of Pd particles and possible absorption and desorption of hydrogen (Bugaev et al., 2013; Skorynina et al., in press) may change the interatomic distances. The same two factors affect the structural disorder of NPs, and therefore, σ^2_{Pd} that includes both thermal and structural disorders cannot be described within correlated Debye model. In addition, E_0 may also be affected by changing the particle size. To account for both Pd–Pd CNs and relative fraction, γ, of Pd atoms transferred to Pd NPs, the latter was derived by the relative decrease of N_{Pd-Cl}, assuming that Pd atoms may be either in (II) or in (0) oxidation state:

$$\gamma = 1 - \frac{1}{1+e^{(T-T_{0,Cl})/\tau_{Cl}}} \quad (2)$$

The obtained evolutions of Pd–N, Pd–Cl and Pd–Pd CNs are shown in Fig. 1b. Since the first two evolutions were obtained according to Eq. (1), they are shown by continuous lines, and not by scatters. Sharp decrease of Pd–Cl contribution takes place at 258 ± 5 °C. Although the decrease of Pd–N CNs bonds is centered at slightly higher temperature (280 ± 10 °C), it is spanned over a wider temperature interval. Thus, loosing of Pd–N bonds starts earlier and their small fraction is still present after formation of Pd NPs, which can be explained by the interaction between surface atoms of Pd NPs with N- and C-atoms of MOF (which cannot be distinguished be EXAFS). In accordance with previous *ex situ* EXAFS, electron microscopy and *in situ* XANES analysis (Bugaev et al.), the Pd–Pd CN at 300 °C is less than its bulk value, which means that Pd NPs are confined within the pores of UiO-67. However, heating to higher temperatures initiated further growth of CN, with final value close to 12 at 450 °C. This means that Pd NPs agglomerate forming bigger particles and most probably destroying crystal structure of UiO-67. To prove the formation of big particles, higher-shell analysis with

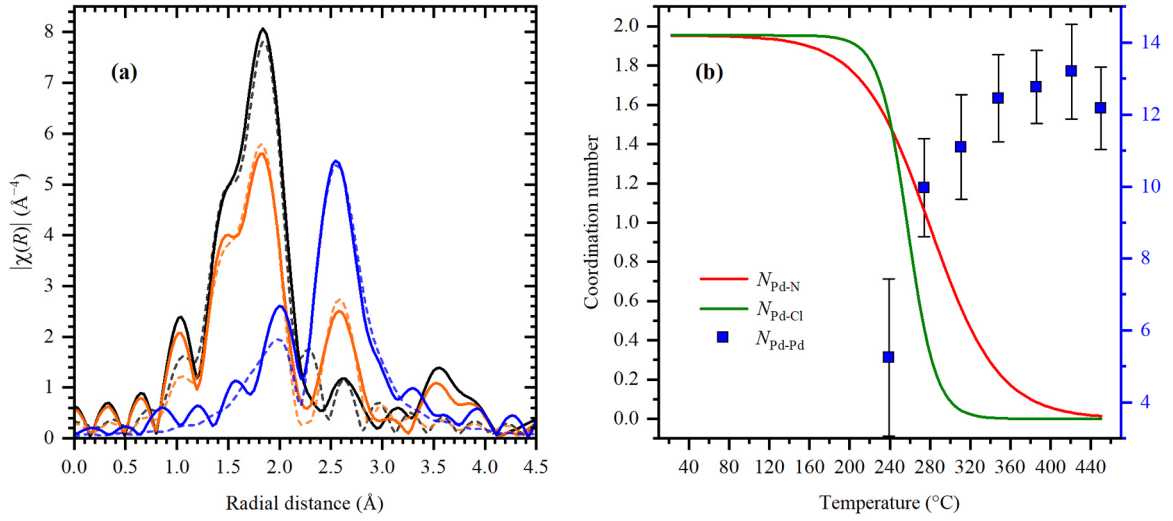

Fig. 1. (a): Experimental phase-uncorrected FT of EXAFS spectra (solid lines) collected during H_2-TPR at RT (black), 239 °C (orange) and 450 °C (blue), with corresponding best fits (dashed lines). (b) The determined dependencies o◯f Pd–N (red line), Pd–Cl (green line) and Pd–Pd (blue squares) CNs.

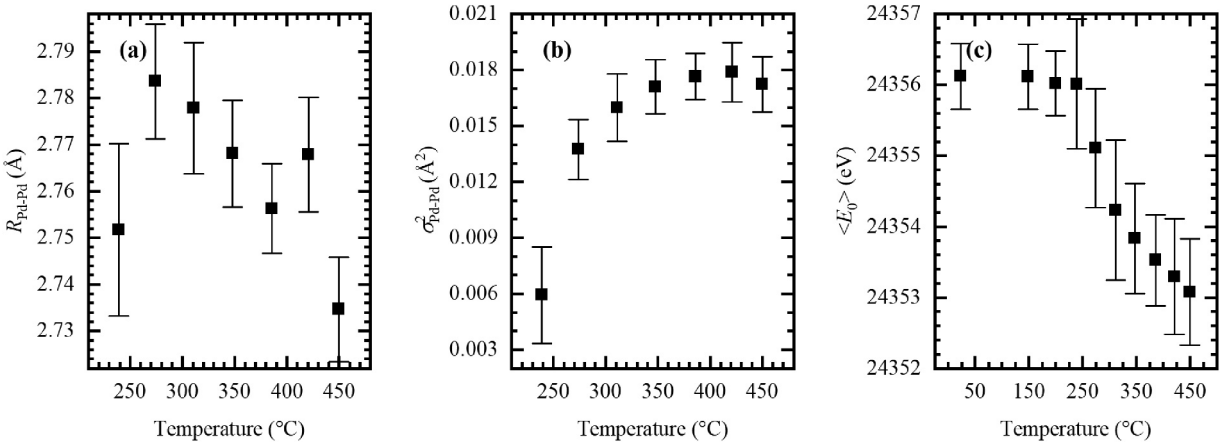

Fig. 2. Temperature-dependence of $R_{Pd\text{-}Pd}$ (a), σ^2_{Pd} (b), and average E_0 value (c) obtained from Fourier-analysis of EXAFS.

the constrains reported in Bugaev et al. (2017) was also performed (see Supporting information).

Fig. 2 summarizes the evolution of Pd–Pd interatomic distances ($R_{Pd\text{-}Pd}$), DW parameter for Pd–Pd contribution (σ^2_{Pd}) and average value of the refined energy of the absorption edge (E_0) (see Eq. (3)). The changes in the $R_{Pd\text{-}Pd}$ values imply that Pd particles are not in pure metallic state except the final point (450 °C) whose $R_{Pd\text{-}Pd}$ is close to that of Pd foil. The behavior of σ^2_{Pd} correlate with the fact of the particle growth. Indeed, if only temperature effects are considered, one should expect a linear increase of DW parameter with temperature (Øien et al., 2015). However, if Pd NPs grow forming bigger particles, the structural disorder becomes lower. As the result, there is no significant increase of σ^2_{Pd} from 300 to 450°C. Finally, the average energy was calculated as

$$\langle E_0 \rangle = \gamma \cdot E_0(Pd^0) + (1-\gamma) \cdot E_0(Pd^{II}) \quad (3)$$

where $E_0(Pd^0)$ and $E_0(Pd^{II})$ are the refined values of zero energy, and γ is calculated according to Eq. (2). This confirms that palladium is reduced from (II) oxidation state to the metallic one.

4. Conclusions

By simultaneous analysis of the series of EXAFS spectra collected during H_2-TPR we have determined the evolution of local atomic structure around Pd atoms in Pd-functionalized UiO-67 MOF. Several important structural results were obtained. (1) In the temperature range from 200 to 300 °C, palladium looses Cl_2 ligands and forms Pd NPs confined inside the pores of UiO-67. (2) Decreasing of the relative number of Pd—N bonds starts at lower temperatures but is spanned over a wider temperature interval in comparison with the decrease of Pd—Cl bonds, explained by the fact that in small Pd NPs interaction of surface Pd atoms with the linkers is not negligible. (3) Heating above 300 °C in hydrogen leads to formation of bigger Pd particles with CN close to that in bulk palladium, which are no longer confined inside UiO-67 pores. (4) The small Pd NPs confined inside UiO-67 pores have much higher structural disorder than bigger Pd particles. The increase of thermal disorder from 300 to 450 °C is compensated by the decrease of structural disorder.

Acknowledgements

We are grateful to Sigurd Øien-Ødegaard and Karl P. Lillerud (University of Oslo) who kindly provided the UiO-67-Pd material investigated in this work and to Kirill Lomachenko for providing the experimental EXAFS data. This research was financial supported by the Russian Science Foundation (Project no. 18-73-00189 to A.L.B., A.A.S. and E.G.L.).

Appendix A. Supplementary material

Supplementary data associated with this article can be found in the online version at doi:10.1016/j.radphyschem.2019.02.003.

References

Bellet, D., Gorges, B., Dallery, A., Bernard, P., Pereiro, E., Baruchel, J., 2003. A 1300 K furnace for in situ X-ray microtomography. J. Appl. Cryst. 36, 366–367. https://doi.org/10.1107/s0021889803001158.

Bordiga, S., Bonino, F., Lillerud, K.P., Lamberti, C., 2010. X-ray absorption spectroscopies: useful tools to understand metallorganic frameworks structure and reactivity. Chem. Soc. Rev. 39, 4885–4927. https://doi.org/10.1039/c0cs00082e.

Borfecchia, E., Braglia, L., Bonino, F., Bordiga, S., Øien, S., Olsbye, U., Lillerud, K.P., van Bokhoven, J.A., Lomachenko, K.A., Guda, A.A., Soldatov, M.A., Lamberti, C., 2017. Probing structure and reactivity of metal centers in metal–organic frameworks by XAS techniques. In: Iwasawa, Y., Asakura, K., Tada, M. (Eds.), XAFS Techniques for Catalysts, Nanomaterials, and Surfaces. Springer, Berlin, pp. 397–430. https://doi.org/10.1007/978-3-319-43866-5_26.

Braglia, L., Borfecchia, E., Lomachenko, K.A., Bugaev, A.L., Guda, A.A., Soldatov, A.V., Bleken, B.T.L., Oien-Odegaard, S., Olsbye, U., Lillerud, K.P., Bordiga, S., Agostini, G., Manzoli, M., Lamberti, C., 2017a. Tuning Pt and Cu sites population inside functionalized UiO-67 MOF by controlling activation conditions. Faraday Discuss. 201, 277–298. https://doi.org/10.1039/c7fd00024c.

Braglia, L., Borfecchia, E., Maddalena, L., Øien, S., Lomachenko, K.A., Bugaev, A.L., Bordiga, S., Soldatov, A.V., Lillerud, K.P., Lamberti, C., 2017b. Exploring structure and reactivity of Cu sites in functionalized UiO-67 MOFs. Catal. Today 283, 89–103. https://doi.org/10.1016/j.cattod.2016.02.039.

Braglia, L., Borfecchia, E., Martini, A., Bugaev, A.L., Soldatov, A.V., Oien-Odegaard, S., Lonstad-Bleken, B.T., Olsbye, U., Lillerud, K.P., Lomachenko, K.A., Agostini, G., Manzoli, M., Lamberti, C., 2017c. The duality of UiO-67-Pt MOFs: connecting treatment conditions and encapsulated Pt species by operando XAS. Phys. Chem. Chem. Phys. 19, 27489–27507. https://doi.org/10.1039/c7cp05185a.

Bugaev, A.L., Guda, A.A., Lomachenko, K.A., Kamyshova, E.G., Soldatov, M.A., Kaur, G., Oien-Odegaard, S., Braglia, L., Lazzarini, A., Manzoli, M., Bordiga, S., Olsbye, U., Lillerud, K.P., Soldatov, A.V., Lamberti, C., 2018. Operando study of palladium nanoparticles inside UiO-67 MOF for catalytic hydrogenation of hydrocarbons. Faraday Discuss. 208, 287–306. https://doi.org/10.1039/c7fd00224f.

Bugaev, A.L., Guda, A.A., Lomachenko, K.A., Shapovalov, V.V., Lazzarini, A., Vitillo, J.G., Bugaev, L.A., Groppo, E., Pellegrini, R., Soldatov, A.V., van Bokhoven, J.A., Lamberti, C., 2017. Core–shell structure of palladium hydride nanoparticles revealed by combined X-ray absorption spectroscopy and X-ray diffraction. J. Phys. Chem. C 121, 18202–18213. https://doi.org/10.1021/acs.jpcc.7b04152.

Bugaev, A.L., Srabionyan, V.V., Soldatov, A.V., Bugaev, L.A., Bokhoven, J.A.V., 2013. The role of hydrogen in formation of Pd XANES in Pd-nanoparticles. J. Phys.: Conf. Ser. 430. https://doi.org/10.1088/1742–6596/430/1/012028.

Butova, V.V., Soldatov, M.A., Guda, A.A., Lomachenko, K.A., Lamberti, C., 2016. Metal-organic frameworks: structure, properties, methods of synthesis and characterization. Russ. Chem. Rev. 85, 280–307. https://doi.org/10.1070/rcr4554.

Cavka, J.H., Jakobsen, S., Olsbye, U., Guillou, N., Lamberti, C., Bordiga, S., Lillerud, K.P., 2008. A new zirconium inorganic building brick forming metal organic frameworks with exceptional stability. J. Am. Chem. Soc. 130, 13850–13851. https://doi.org/10.1021/ja8057953.

Chavan, S., Vitillo, J.G., Gianolio, D., Zavorotynska, O., Civalleri, B., Jakobsen, S., Nilsen, M.H., Valenzano, L., Lamberti, C., Lillerud, K.P., Bordiga, S., 2012. H_2 storage in isostructural UiO-67 and UiO-66 MOFs. Phys. Chem. Chem. Phys. 14, 1614–1626. https://doi.org/10.1039/c1cp23434j.

Øien, S., Agostini, G., Svelle, S., Borfecchia, E., Lomachenko, K.A., Mino, L., Gallo, E., Bordiga, S., Olsbye, U., Lillerud, K.P., Lamberti, C., 2015. Probing reactive platinum

sites in UiO-67 zirconium metal–organic frameworks. Chem. Mater. 27, 1042–1056. https://doi.org/10.1021/cm504362j.

Ravel, B., Newville, M., 2005. Athena, Artemis, Hephaestus: data analysis for X-ray absorption spectroscopy using Ifeffit. J. Synchrotron Radiat. 12, 537–541. https://doi.org/10.1107/S0909049505012719.

Skorynina, A.A., Tereshchenko, O.A., Usoltsev, A.L., Bugaev, K.A., Lomachenko, A.A., Guda, E., Groppo, R., Pellegrini, C., Lamberti, A.V., Soldatov Time-dependent carbide phase formation in palladium nanoparticles. Radiat. Phys. Chem. doi: 10.1016/j.radphyschem.2018.11.033. (in press).

Soldatov, M.A., Martini, A., Bugaev, A.L., Pankin, I., Medvedev, P.V., Guda, A.A., Aboraia, A.M., Podkovyrina, Y.S., Budnyk, A.P., Soldatov, A.A., Lamberti, C., 2018. The insights from X-ray absorption spectroscopy into the local atomic structure and chemical bonding of metal–organic frameworks. Polyhedron 155, 232–253. https://doi.org/10.1016/j.poly.2018.08.004.

Wang, Z., Cohen, S.M., 2009. Postsynthetic modification of metal-organic-frameworks. Chem. Soc. Rev. 38, 1315–1329. https://doi.org/10.1039/b802258p.